Low-Temperature Diffusion at Ni/SiC Interface with the Aid of Femtosecond Laser-Induced Strain

Yusuke Takidani[*1], Kazuki Morimoto[*1], Kenta Kondo[*1], Tomoyuki Ueki[*2], Takuro Tomita[*2], Yasuhiro Tanaka[*3] and Tatsuya Okada[*2]

[*1] *Graduate School of Advanced Technology and Science, Tokushima University, 2-1 Minamijosanjima, Tokushima 770-8506, Japan*
[*2] *Institute of Technology and Science, Tokushima University, 2-1 Minamijosanjima, Tokushima 770-8506, Japan*
E-mail: tatsuya-okada@tokushima-u.ac.jp
[*3] *Deparment of Advanced Materials Science, Faculty of Engineering, Kagawa University, 2217-20 Hayashi-cho, Takamatsu 761-0396, Japan*

We investigated low-temperature annealing of the Ni/SiC system in which a laser-modified strained region was introduced in the SiC before annealing. The objective was to identify the Ni-silicide phase, and to characterize the spatial distribution of carbon atoms. A Ni film with a nominal thickness of 500 nm was deposited on an n-type SiC substrate. The Ni/SiC interface was irradiated by femtosecond laser pulses to introduce the strained region. The laser light was incident on the interface through SiC, which is transparent to the femtosecond laser. Annealing was carried out at 573 K or 673 K. Micro-Raman spectroscopy detected amorphous carbon only on the Ni surface annealed at 673 K for 60 s. On the Ni surface annealed at 573 K for 60 s, carbon was not detected irrespective of laser-irradiation at the interface. This difference was thought to be due to the large difference in the carbon diffusion length in Ni at these annealing conditions. To identify the composition of nickel silicide, such as NiSi, $NiSi_2$, and Ni_2Si, we analyzed selected area diffraction patterns in transmission electron microscopy. The Ni-silicide phase at the Ni/SiC interface was identified as NiSi.

DOI: 10.2961/jlmn.2015.03.0014
Keywords: Ni/SiC interface, femtosecond laser, strain, annealing, diffusion

1. Introduction

Silicon carbide (SiC) is a compound semiconducting material with very strong atomic bonds between the silicon (Si) and carbon (C) atoms. The tight Si-C bonding gives SiC a wide bandgap and very high breakdown electric field. It also yields high-energy optical phonons, leading to a high saturated electron drift velocity and high thermal conductivity. These physical properties make SiC a promising candidate for high-temperature, high-power and high-frequency devices, which cannot be realized with conventional Si-based materials [1]. For example, the wide bandgap and superior thermal stability ensure suitability for high-temperature application. High-power and high-frequency applications derive directly from high breakdown field and high saturated electron drift velocity, respectively.

Before practical SiC-based devices can be fabricated, however, some technological problems remain to be solved. One has to do with the fabrication of high-quality ohmic contacts on SiC. For reliable metal/SiC contacts, not only low electric resistivity but also high thermal stability is required for high-temperature application. The conventional method for contact formation on n-type SiC involves high-temperature annealing at above 1073 K after the deposition of a thin film of nickel (Ni) [2-16]. Ni acts as a catalyst to break the strong Si-C bonds at high annealing temperatures, and combines with Si to form various types of Ni-silicide at the Ni/SiC interface. With longer annealing times, Ni is consumed and completely compensated by Ni-silicide. In some cases, C atoms separate from the SiC and diffuse through the Ni (or Ni-silicide) film to reach the film surface.

No commonly accepted theory has yet been established as to the formation mechanisms of low-resistivity contacts in the Ni/SiC system. However, many researchers have claimed that the distribution and chemical state of C atoms play an important role in the contact formation [13,15-20]. From a practical point of view, some researchers have pointed out that free C atoms might have an adverse effect on the long-term durability of the contacts [21]. In addition, the thermal stability of Ni/SiC contacts might also be affected by the type of Ni-silicide formed at the Ni/SiC interface [22]. Therefore, structural analyses (i.e., the identification of C distribution and type of Ni-silicide) are of great importance in the study of Ni/SiC contacts.

Femtosecond (fs) laser is a light source that can generate laser pulses with very short duration, around 100 fs. It is known that regions modified by a femtosecond laser are two orders of magnitude smaller than regions modified using other types of lasers, such as nanosecond or continuous wave lasers. Since the thermal diffusion length of a femtosecond laser (~ 2 nm) is much smaller than the minimum processing size (~ 1 μm), the thermal effect associated with femtosecond laser processing is practically negligible. Hence, the intense optical electric field of a femtosecond laser light can break the chemical bond in a material in

an athermal manner. When femtosecond laser pulses are irradiated inside a transparent material, multi-photon absorption takes place at the focal point. The electrons generated in the conduction band by the multi-photon absorption are accelerated by the electric field of laser light, which triggers avalanche ionization of the material. The crystal lattice is destabilized by the vast amount of electrons generated through the process, which leads to the modification of the material.

We have been studying the femtosecond laser-induced modification of SiC single crystals [23-29]. Femtosecond laser irradiation inside a SiC single crystal induces the formation of a strained region composed of quasi-periodic strained layers with high residual stress around 1 GPa [25,26,28]. Recently, we reported that femtosecond laser-induced strain can be applied to enhance atomic diffusion at the Ni/SiC interface annealed at relatively low temperatures [29]. Irradiation with femtosecond laser pulses at the Ni/SiC interface induced the formation of a strained region in the SiC crystal adjacent to the interface. After annealing at temperatures in the range of 573-723 K, preferential Ni diffusion towards the strained region in SiC was clearly visualized by transmission electron microscopy (TEM) / electron energy loss spectroscopy (EELS) element mapping. Concurrently, Si and C diffused in the opposite direction, that is, towards the Ni film. As a consequence, an interdiffusion layer was formed at the Ni/SiC interface. Such interdiffusion was not found in the region without femtosecond laser-induced modification in SiC. Hence, it is clear that the femtosecond laser-induced modification of SiC enhanced interdiffusion in the Ni/SiC system annealed at relatively low temperatures.

The major objective of the present study was to detect C migration using micro-Raman spectroscopy. Another objective was to identify the Ni-silicide at the Ni/SiC interface using TEM/selected area diffraction (SAD) analysis. Such knowledge about carbon and Ni-silicide would serve to provide insight into the potential application of femtosecond laser-assisted low-temperature annealing to the Ni/SiC contact formation.

2. Experimental procedures

n-type SiC (0001) 8°-off single crystal wafers of 4H- and 6H-structures were used as a substrate. The surface oxide was removed by etching in a 10-15 vol.% HF solution in distilled water. Before and after etching, ultrasonic cleaning was carried out in acetone, ethanol and distilled water. A Ni film with a nominal thickness of 500 nm was deposited on the Si surface of the SiC crystal using electron beam evaporation in a high vacuum. SiC is transparent to the laser light of wavelength 800 nm. To introduce strained regions in the SiC crystal adjacent to the Ni/SiC interface, femtosecond laser pulses irradiated the Ni/SiC interface from the transparent SiC side as the sample stage moved at a scan speed of 50 μm/s. The light source was a 1-kHz Ti:sapphire regenerative amplifier, based on a chirped pulse amplification system, operating at 800 nm (Spectra-Physics, Spitfire). The electric field of laser light was kept parallel to the major irradiation lines; Figure 1 is a schematic illustration of the procedure. The distance between the major irradiation lines was controlled to be 10 μm or 2.5 μm. The wavelength, pulse width, and frequency were 800 nm, 130 fs and 1 kHz, respectively. The pulse energy was 2 μJ/pulse, which corresponds to a fluence of 30 J/cm^2 at the Ni/SiC interface [29]. After the laser irradiation, annealing was carried out in a vacuum using an infrared radiation heating apparatus. The heat-up time was 60 s. The tip of a thermocouple was kept in contact with the samples. The conditions of femtosecond laser-irradiation and annealing for each sample are summarized in Table 1.

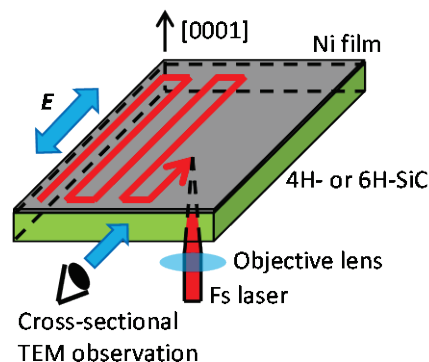

Fig. 1 Schematic of laser irradiation. The focused laser light is incident on the Ni/SiC interface through the transparent SiC substrate. The electric field (***E***) is parallel to the major irradiation lines. Cross-sectional TEM observations are made parallel to the major irradiation line.

Table 1 Experimental conditions

	Substrate	Line spacing	Annealing	Raman analysis	TEM Sample preparation
A	6H-SiC	-	-	-	Ar-ion
B	6H-SiC	2.5 μm	573K-60s	○	-
C	6H-SiC	2.5 μm	673K-60s	○	FIB
D	4H-SiC	10 μm	573K-600s	-	Ar-ion

Micro-Raman spectroscopy was carried out to detect C atoms that migrated to the Ni surface, with a Renishaw inVia Reflex-S. The wavelength of Raman excitation was 532 nm, and the excitation power was 7.5 mW. The exposure time was 5 s for each measurement point.

Two different TEM sample preparation techniques were adopted to observe the cross-section. The first was a method that used Ar-ion milling for the final thinning process. The annealed sample was cut into halves perpendicularly to the major irradiation lines and glued together at the Ni sides between two dummy SiC pieces to make a raft-like sample. This sample was then mechanically thinned and subsequently dimpled. The final thinning was carried out by Ar ion-milling until a small perforation was made in the center. The second TEM sample preparation technique was the Ga focused ion beam (FIB) pick-up method, that used a FEI Quanta 3D 200i equipped with the Omniprobe pick-up system. In this method, after depositing a Pt protection layer on the Ni surface, two trenches were made, leaving a rectangular thin "wall" (10×5×2 μm^3) between the trenches. Three sides of the wall were then cut off from the surrounding, leaving a very small portion at one corner. The wall was welded to a sharp pick-up probe, and the remaining corner was cut. The picked-up wall was welded to the side surface of a pillar in a lift-out grid, and then the connection between the probe and wall was cut. The final thin-

ning was made parallel to the wall surface until we obtained an electron-transparent sample of 10 μm×5 μm×100-200 nm. The sample volume necessary for the FIB method was considerably smaller than that needed for the Ar ion-milled one. Other advantages of the FIB method include its site-specific nature and high success rate. The major disadvantage, however, is the damage that the ion beam of Ga inevitably inflicts on the sample surface. The amorphous layer on a FIB-prepared TEM sample is considerably thicker than that on an Ar ion-milled sample surface. In the present study, we used the Ar-ion milling technique to prepare the samples to observe the SAD pattern in order to avoid the effect of the surface amorphous layer.

TEM observations were made with a JEOL JEM-2100F microscope operated at 200 kV in the scanning transmission electron microscopy (STEM) mode.

In the present study, we report results for four Samples, A-D. As will be described, Sample A was the as-Ni deposited sample to observe the state without the effect of laser-irradiation and annealing.

3. Results

3.1 Sample A

A cross-sectional TEM sample was prepared from Sample A in which a Ni film with a nominal thickness of 500 nm was deposited on a 6H-SiC substrate. A STEM dark-field image of the sample is shown in Fig. 2(a). In a dark-field STEM image, regions containing lighter atoms appear darker, due to weaker electron scattering by the atoms. Hence, the SiC substrate appears darker than the Ni film in Fig. 2(a). The Ni/SiC interface is flat, and no crystallographic defect is observed in the SiC substrate. The weak contrast in the Ni film suggests that the film is polycrystalline. Figure 2(b) shows a SAD pattern taken at the Ni/SiC interface. The pattern consists of a regular arrangement of diffraction spots from single-crystalline SiC, and Debye rings from polycrystalline Ni. From the spot pattern, it was confirmed that the electron beam was incident from the $[11\bar{2}0]$ direction of SiC. The four rings visible in the pattern correspond to the {111}, {200}, {220}, and {311} planes of Ni. The radii of the rings agree with the calculated values from the inter-planar spacing of Ni within a margin of error of 2.6%.

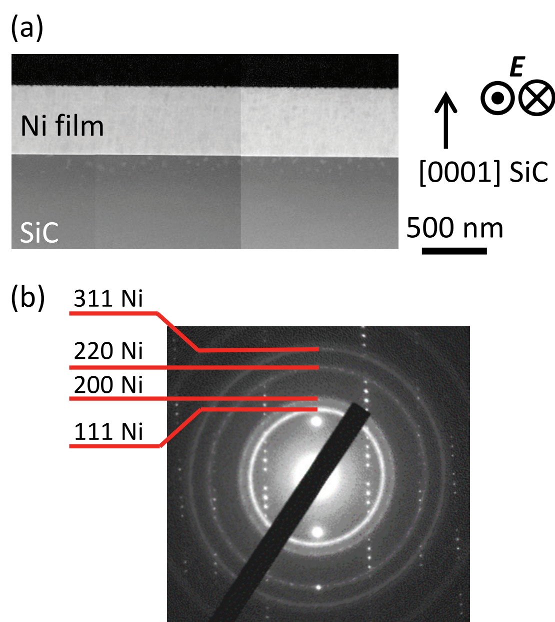

Fig. 2 (a) Cross-sectional STEM dark-field image of Sample A. **(b)** Selected area diffraction pattern taken at the Ni/SiC interface. The crystallographic indices of the first four Debye rings of polycrystalline Ni are shown.

3.2 Sample B

As shown in Table 1, the spacing between major femtosecond laser-irradiation lines in Sample B was 2.5 μm. Since this spacing was smaller than the average width of the laser-modified region associated with each irradiation line (approximately 7 μm), it was expected that the SiC adjacent to the Ni/SiC interface would be completely laser-modified. The annealing was carried out at 573 K for 60 s. An optical micrograph of the sample surface is shown in Fig. 3(a). Although the femtosecond laser-irradiation was made from the transparent SiC side, it is obvious that the Ni surface has considerable laser-induced undulation. A micro-Raman analysis was conducted at the boundary between the undulated and flat surfaces. Typical Raman spectra are shown in Figs. 3(b) and (c). Neither spectra has a

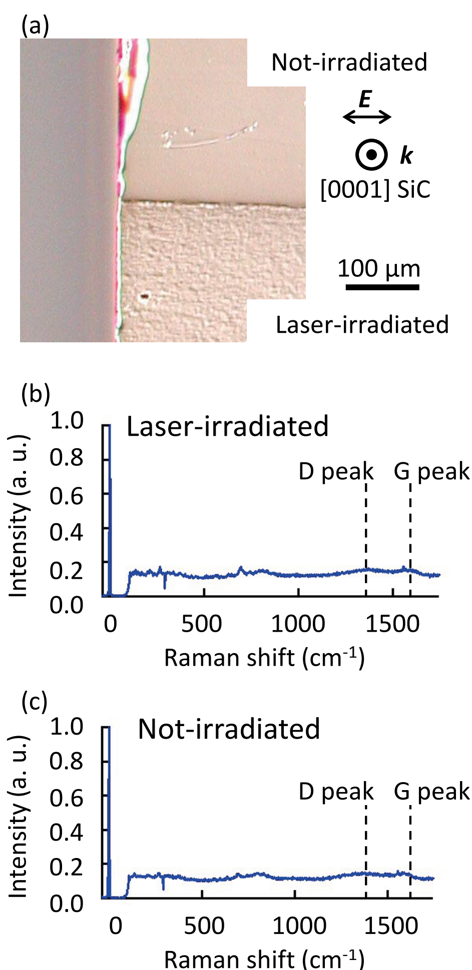

Fig. 3 (a) Optical micrograph of the Ni surface of Sample B. Although the laser-irradiation was made from the SiC side, the laser-irradiated area of the Ni film surface shows undulation. **(b)** Raman spectrum taken from the undulated surface (i.e., laser-irradiated area). **(c)** Raman spectrum taken from the flat surface (i.e., not-irradiated area).

peak at D (1350 cm^{-1}) or G (1580 cm^{-1}), positions ascribed to amorphous C (a-C). It is clear that there is practically no difference between the two profiles. Thus the Ni surface was not covered by C atoms under the annealing condition of 573 K for 60 s.

3.3 Sample C

As shown in Table 1, the laser-irradiation condition of Sample C was the same as that of Sample B. The annealing was carried out at 673 K for 60 s, 100 K higher than that of Sample B. Figure 4(a) is a STEM dark-field image of the cross-sectional sample prepared by the FIB pick-up method. The bottom dark region in the micrograph corresponds to the SiC substrate. The second layer from the bottom is the Ni film, covered by the Pt protective layer deposited prior to the FIB micro-trenching. As shown in Fig. 4(b), laser-induced modification was found in the SiC substrate adjacent to the Ni/SiC interface. A thin interlayer, approximately 50-nm thick, was found between the Ni film and SiC substrate, which corresponded to the interdiffusion layer of Ni, Si, and C. However, the extent of C diffusion into the Ni film was not determined solely from the STEM image contrast. Even if we had applied TEM/EELS analysis to the sample, the sensitivity and spatial resolution would have been too restricted to detect the very low C concentration in the Ni film. Hence, we applied micro-Raman spectroscopy to verify C atoms on the Ni film surface.

Typical Raman spectra are shown in Figs. 5(a) and (b) for the areas with/without laser-induced surface undulation, respectively. Although a-C peaks are not visible in the area without laser-induced undulation [Fig. 5(b)], both D and G broad peaks can be clearly observed in the undulated surface [Fig. 5(a)]. Figure 5(c) is a mapping of the G peak intensity at the boundary between the flat and undulated surfaces. It is clear that the peak intensity drastically changes at the boundary. C atoms exist only on the surface of the laser-modified region.

The results of micro-Raman spectroscopy strongly suggest that the separated C atoms from the Si-C bonding diffused vertically towards the Ni surface. There is also an indication that this reaction occurred predominantly at the interface irradiated by femtosecond laser prior to low-temperature annealing. In addition, a comparison of Samples B and C, which underwent the same laser-irradiation condition, indicates that the annealing condition is critical to the C diffusion, because surface C was detected only on the top of the laser-irradiated area in Sample C.

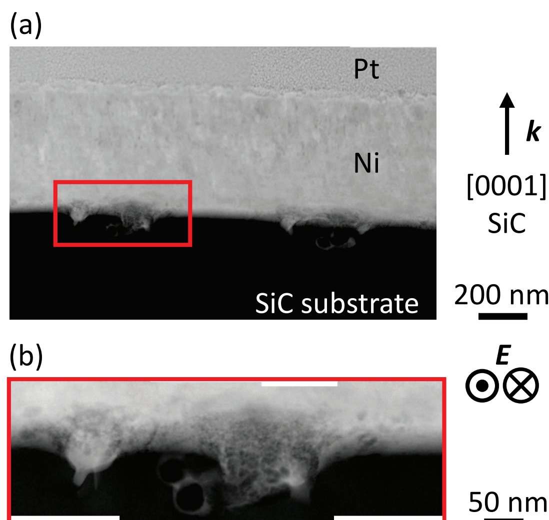

Fig. 4 (a) Cross-sectional STEM dark-field image of Sample C. **(b)** An enlarged image of the rectangular area in **(a)**.

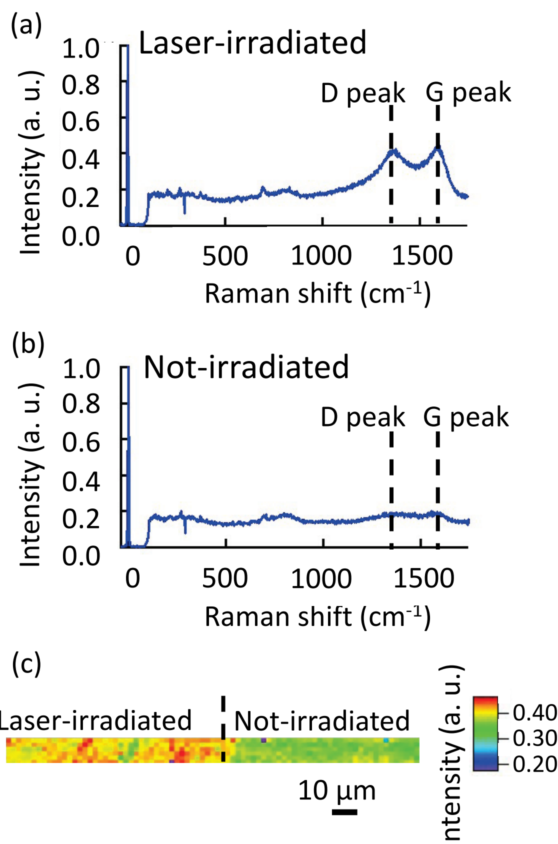

Fig. 5 (a) Raman spectrum taken from the undulated surface (i.e., laser-irradiated area) of Sample C. **(b)** Raman spectrum taken from the flat surface (i.e., not-irradiated area). **(c)** Mapping made from the intensity of the G position (1580 cm^{-1}) in Raman spectrum.

3.4 Sample D

As shown in Table 1, 4H-SiC was used as substrate in Sample D. The spacing between the major laser-irradiation lines was 10 μm, larger than the average width of the laser-modified region associated with each irradiation line (7 μm). The annealing was carried out at 573 K for 600 s. The longer annealing time was chosen to promote the development of an interdiffusion layer at the Ni/SiC interface. The cross-sectional TEM sample was prepared by the Ar-ion milling. A STEM dark-field image of the Ni/SiC interface is shown in Fig. 6(a). Quasi-periodic laser-induced modification is seen in the SiC substrate adjacent to the interface. Between the Ni film and SiC substrate, an interlayer of approximately 100-nm thickness is clearly visible, which corresponds to the interdiffusion layer of Ni, Si, and C. It is also clear that the interdiffusion occurred predominantly towards the quasi-periodically arranged laser-modification in SiC. Well-developed interdiffusion layer was observed adjacent to the laser-induced strained regions in the SiC substrate. The Ni/SiC interface between strained regions

remained flat and undisturbed even after annealing at 573 K for 600 s.

A SAD pattern taken at the boundary between the interlayer and SiC substrate is shown in Fig. 6(b). In addition to the diffraction spots from the 4H-SiC single crystal, spots were found arranged on broken rings. We calculated the inter-planar spacing from the radii of the rings to compare with the values in Ni-silicide, such as NiSi, Ni_2Si and $NiSi_2$. The rings in Fig. 6(b) were found to correspond to the {111}, {200}, {210}, {211}, and {220} planes in NiSi, respectively. The Ni-silicide formed under the annealing temperature 573 K was identified as the NiSi phase. It is known that the NiSi phase is a precursor to the thermodynamically stable Ni_2Si phase [19,22]. A longer annealing time might be considered to form thermally stable Ni/SiC contact through the present low-temperature process.

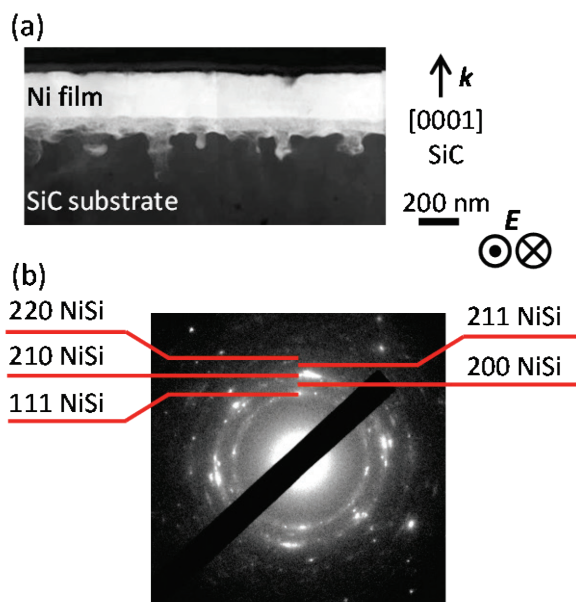

Fig. 6 (a) Cross-sectional dark-field image of Sample D. **(b)** Selected area diffraction pattern taken at the interface between interlayer and SiC. The crystallographic indices of the first five broken rings of polycrystalline NiSi are shown.

4. Discussion

In the present study, micro-Raman spectroscopy was applied to detect C atoms on the Ni surface. C was not detected in Sample C annealed at 573 K for 60 s. On the other hand, C atoms diffused to the Ni surface in the laser-irradiated area of Sample D, annealed at 673 K for 60 s. In the following, we estimate the C diffusion length in Ni for these annealing conditions.

The diffusion length is roughly estimated to be $\sqrt{Dt}$, where t is the annealing duration. The diffusion coefficient D follows the Arrhenius-type equation, $D = D_0 \exp(-Q/RT)$, where D_0 is the temperature-independent constant, Q is the activation energy, R is the gas constant, and T is the thermodynamic temperature. If we use 1.2×10^{-5} m^2/s and 137 kJ/mol for D_0 and Q, respectively, for C diffusion in Ni, we obtain 15 nm and 130 nm for 60 s - annealing at 573 K and 673 K, respectively. Considering that reliable data for D_0 and Q are available only in a high temperature range (873-1673 K), this rough estimation is enough to explain the different C diffusion behavior in Samples B and C, although the estimated diffusion length of 130 nm is smaller than the nominal thickness of Ni film, 500 nm.

5. Summary

We carried out micro-Raman spectroscopy and cross-sectional TEM/SAD analysis to study the C diffusion and Ni-silicide formation associated with low-temperature annealing of the Ni/SiC system with femtosecond laser-induced strain. The Ni/SiC interface was irradiated by femtosecond laser pulses from the SiC side to introduce the strained region, and then annealed at 573 K or 673 K. Micro-Raman spectroscopy detected a-C only at the top of Ni film annealed at 673 K, under which the Ni/SiC interface was laser-irradiated. The result supports the idea that femtosecond laser-induced strain in the near-interface region in SiC helps to break Si-C bonding at relatively low annealing temperatures, leading to interdiffusion among Ni, Si, and C atoms, and that the separated C atoms diffuse towards the Ni film surface in a short time duration. The TEM/SAD analysis identified the Ni-silicide formed at the Ni/SiC interface as the NiSi phase.

Acknowledgments

This work was supported by JSPS KAKENHI Grant-in-Aid for Challenging Exploratory Research, Grant Number 26630132 and THE AMADA FOUNDATION.

References

[1] H. Matsunami and T. Kimoto: Mater. Sci. Eng. R, 20, (1997) 125.
[2] T. Uemoto: Jpn. J. Appl. Phys. Part 2, 34, (1995) L7.
[3] J. Crofton, P.G. McMullin, J.R. Williams and M.J. Bozack: J. Appl. Phys., 77, (1995) 1317.
[4] Ts. Marinova, V. Krastev, C. Hallin, R. Yakimova and E. Janzen: Appl. Surf. Sci., 99, (1996) 119.
[5] Ts. Marinova, A. Kakanakova-Georgieva, V. Krastev, R. Kakanakov, M. Neshev, L. Kassamakova, O. Noblanc, C. Arnodo, S. Cassette, C. Brylinski, B. Pecz, G. Radnoczi and Gy. Vincze: Mater. Sci. Eng. B, 46, (1997) 223.
[6] M.G. Rastegaeva, A.N. Andreev, A.A. Petrov, A.I. Babanin, M.A. Yagovkina and I.P. Nikitina: Mater. Sci. Eng. B, 46, (1997) 254.
[7] B. Pécz, G. Radnóczi, S. Cassette, C. Brylinski, C. Arnodo and O. Noblanc: Diamond Relat. Mater., 6, (1997) 1428.
[8] A. Kakanakova-Georgieva, Ts. Marinova, O. Noblanc, C.Arnodo, S. Cassette and C. Brylinski: Thin Solid Films, 343-344, (1999) 637.
[9] F. Roccaforte, F. La Via, V. Raineri, L. Calcagno and P. Musumeci: Appl. Surf. Sci., 184, (2001) 295.
[10] S.Y. Han, K.H. Kim, J.K. Kim, H.W. Jang, K.H. Lee, N.K. Kim, E.D. Kim and J.L. Lee: Appl. Phys. Lett., 79, (2001) 1816.
[11] S.Y. Han, J.Y. Shin, B.T. Lee and J.L. Lee: J. Vac, Sci. Technol. B, 20, (2002) 1496.
[12] F. La Via, F. Roccaforte, A. Makhtari, V. Raineri, P. Musumeci and L. Calcagno: Microelectron. Eng., 60, (2002) 269.

[13] F. La Via, F. Roccaforte, V. Raineri, M. Mauceri, A. Ruggiero, P. Musumeci, L. Calcagno, A. Castaldini and A. Cavallini: Microelectron. Eng., 70, (2003) 519.
[14] I.P. Nikitina, K.V. Vassilevski, N.G. Wright, A.B. Horsfall, A.G. O'Neill and C.M. Johnson: J. Appl. Phys., 97, (2005) 083709.
[15] M. Siad, C. Pineda Vargas, M. Nkosi, D. Saidi, N. Souami, N. Daas and A.C. Chami: Appl. Surf. Sci., 256, (2009) 256.
[16] M. Siad, M. Abdesslam and A.C. Chami: Appl. Surf. Sci., 258, (2012) 6819.
[17] I. Ohdomari, S. Sha, H. Aochi, T. Chikyow and S. Suzuki: J. Appl. Phys., 62, (1987) 3747.
[18] M.G. Rastegaeva, A.N. Andreev, A.A. Petrov, A.I. Babanin, M.A. Yagovkina and I.P. Nikitina: Mater. Sci. Eng. B, 46, (1997) 254.
[19] A. Bächli, M.A. Nicolet, L. Baud, C. Jaussaud and R. Madar: Mater. Sci. Eng. B, 56, (1998) 11.
[20] W. Lu, W.C. Mitchel, G.R. Landis, T.R. Crenshaw and W.E. Collins: Solid State Electron., 47, (2003) 2001.
[21] P. Macháč, B. Barda and J. Maixner: Appl. Surf. Sci., 254, (2008) 1691.
[22] S. Kim, J.H. Perepezko, Z. Dong and A.S. Edelstein: J. Electron. Mater., 33, (2004) 1064.
[23] T. Tomita, K. Kinoshita, S. Matsuo and S. Hashimoto: Appl. Phys. Lett., 90, (2007) 153115.
[24] T. Okada, H. Kawahara, Y. Ishida, R. Kumai, T. Tomita, S. Matsuo, S. Hashimoto, M. Kawamoto, Y. Makita and M. Yamaguchi: Appl. Phys. A, 92, (2008) 665.
[25] T. Okada, T. Tomita, S. Matsuo, S. Hashimoto, Y. Ishida, S. Kiyama and T. Takahashi: J. Appl. Phys., 106, (2009) 054307.
[26] M. Yamamoto, M. Deki, T. Takahashi, T. Tomita, T. Okada, S. Matsuo, S. Hashimoto, M. Yamaguchi, K. Nakagawa, N. Uehara and M. Kamano: Appl. Phys. Express, 3, (2010) 016603.
[27] T. Tomita, T. Okada, H. Kawahara, R. Kumai, S. Matsuo, S. Hashimoto, M. Kawamoto, M. Yamaguchi, S. Ueno, E. Shindou and A. Yoshida: Appl. Phys. A, 100, (2010) 113.
[28] T. Okada, T. Tomita, S. Matsuo, S. Hashimoto, R. Kashino and T. Ito: Mater. Sci. Forum, 725, (2012) 19.
[29] T. Ueki, K. Morimoto, H. Yokota, T. Tomita and T. Okada: Appl. Phys. Express, 8, (2015) 026503.

(Received: May 23, 2015, Accepted: November 26, 2015)